ELSEVIER

Journal of Hepatology 49 (2008) 441–450

Journal of Hepatology

www.elsevier.com/locate/jhep

Fish oil fed prior to ethanol administration prevents acute ethanol-induced fatty liver in mice☆

Satoshi Wada[1,2], Tomomi Yamazaki[1,*], Yukari Kawano[2], Shinji Miura[1], Osamu Ezaki[1,*]

[1]*Nutritional Science Program, National Institute of Health and Nutrition, 1-23-1, Toyama, Shinjuku-ku, Tokyo 162-8636, Japan*
[2]*Department of Food and Nutritional Science, Graduate School of Agriculture, Tokyo University of Agriculture, 1-1-1 Sakuraoka, Setagaya-ku, Tokyo 156-8502, Japan*

***Background/Aims*: We examined whether dietary fish oil can prevent acute ethanol (alcohol)-induced fatty liver.**

***Methods*: Mice were fed safflower oil, fish oil, or safflower oil plus a PPARα activator on the day prior to ethanol administration. Oil red O staining, serum analysis, and RT-PCR were used to analyze ethanol-induced fatty liver.**

***Results*: In mice fed safflower oil, ethanol increased liver TG 3-fold, with activation of SREBP-1c and ChREBP, which promote *de novo* lipogenesis, and increases in expression of mRNAs for PPARγ and DGATs mRNAs, which promote TG synthesis. When mice were fed fish oil, ethanol-induced fatty liver was reduced by 73%. Fish oil decreased SREBP-1c activity and increased PPARα activity. However, levels of DGAT1, DGAT2, ChREBP, LPK, and PPARγ mRNAs were increased in response to ethanol in mice fed fish oil. Prior administration of Wy14643, PPARα activator, did not inhibit ethanol-induced fatty liver, suggesting that PPARα played little role in prevention of ethanol-induced fatty liver by fish oil.**

***Conclusions*: A single dose of ethanol increases the liver TG level via several mechanisms; however, prior ingestion of fish oil effectively prevents ethanol-induced fatty liver, at least in part, by decreasing basal SREBP-1c activity, especially a marked reduction in SCD1.**

***Keywords*: n-3 fatty acids; Liver steatosis; SCD1; CD36; Docosahexaenoic acid; Sterol regulatory element-binding protein; Alcohol; Fatty liver; Fish oil; Ethanol; Steatosis**

1. Introduction

Alcoholic liver disease is a major cause of illness and death in affluent countries. In the initial stages of the disease, accumulation of fat in hepatocytes leads to development of fatty liver (steatosis). If alcohol consumption is continued, steatosis may progress to hepatitis and fibrosis, which may lead to liver cirrhosis. Reducing or preventing accumulation of fat within the liver in response to alcohol consumption may block or delay the progression of fatty liver to hepatitis and fibrosis. Therefore, it is important to understand the biochemical and molecular mechanisms that underlie fat accumulation and to understand how dietary factors modulate this fat accumulation in liver [1].

Administration of a single dose of ethanol to a rat causes fatty liver. This animal model has physiologic characteristics comparable to those of binge drinking in humans [2]. The mechanism underlying development of fatty liver in response to acute ethanol administration was first described more than 40 years ago. Accumulation of triglycerides (TG) is attributed to a stimulatory effect of ethanol on the biosynthesis of fatty acids by

Received 1 February 2008; received in revised form 22 March 2008; accepted 9 April 2008; available online 11 June 2008
Associate Editor: C.P. Day

☆ The authors declare that they do not have anything to disclose regarding funding from industries or conflict of interest with respect to this manuscript.

* Corresponding authors. Tel.: +81 3 3203 5725; fax: +81 3 3207 3520.

E-mail addresses: tomo0322@nih.go.jp (T. Yamazaki), ezaki@nih.go.jp (O. Ezaki).

0168-8278/$34.00 © 2008 European Association for the Study of the Liver. Published by Elsevier B.V. All rights reserved.
doi:10.1016/j.jhep.2008.04.026

the liver [3] and/or increased mobilization fatty acids from adipose tissue [4]. However, the rat model of acute ethanol-induced fatty liver has not been studied widely since the initial description.

In contrast, the mechanisms of the chronic effects of ethanol have been studied extensively. A transcription factor, sterol regulatory element-binding protein (SREBP)-1c that regulates lipogenesis in the liver [5] may contribute to development of fatty liver in response to chronic alcohol administration. C57BL/6J mice fed ethanol in a liquid diet for 4 weeks showed an increase in the mature (active) form of SREBP-1 and expression of its target lipogenic genes [6]. SREBP-1c-null mice fed ethanol by intragastric infusion for 4 weeks showed a small increase in the liver TG concentration (13.4 mg/g liver), whereas wild-type mice showed a marked increase in liver TG (64.9 mg/g liver) in response to ethanol [7]. Another transcription factor, peroxisome proliferator-activated receptor (PPAR) α, which increases β oxidation of fatty acids [8], may also contribute to ethanol-induced fatty liver. Ethanol inhibited PPARα activation of expression of a reporter gene in hepatoma cells [9]. Administration of Wy14643 (0.1%), a PPARα agonist, prevented fatty liver in mice fed ethanol as a liquid diet for 4 weeks [10]. However, the chronic effects of such agents on mice fed ethanol might be affected by metabolic alterations induced indirectly by long-term ethanol administration.

Dietary fish oil might be useful for preventing ethanol-induced fatty liver. Fish oil contains n-3 fatty acids, such as eicosapentaenoic acid and docosahexaenoic acid, which decrease blood TG concentrations in hypertriglycemic patients and are thought to have protective effects against fatty liver [11]. These effects are due mainly to the combined effects of inhibition of lipogenesis by inactivation of SREBP-1c and stimulation of fatty-acid oxidation by activation of PPARα in the liver [12,13]. In the present study, we examined the mechanism underlying development of fatty liver in response to acute ethanol administration and examined whether prior fish oil feeding can prevent this type of fatty liver.

2. Materials and methods

2.1. Animals

Eight-week-old male C57BL/6 mice were purchased from Tokyo Laboratory Animal Science (Tokyo, Japan). They were fed a normal laboratory diet (CE2, Clea, Tokyo, Japan) for 1 week to stabilize metabolic conditions. Mice were exposed to a 12-h light/12-h dark cycle and maintained at a constant temperature of 22 °C. Four mice were housed per plastic cage equipped with plastic partitions to separate individual mice. Mice were cared for in accordance with the NIH Guide for the Care and Use of Laboratory Animals. All animal experiments were conducted with approval of National Institute of Health and Nutrition Ethics Committee on Animal Research (No. 0606).

2.2. Ethanol administration

At 7 a.m., food was removed and mice were fasted. At 9 a.m., a solution of ethanol in water (40% volume/volume) was administered intragastrically. As a control, a glucose solution (40% weight/volume) that contained the same energy as the ethanol solution was given. In time-course studies, ethanol was administrated at a dose of 3 g/kg body weight (volume is 200–250 μL/mouse), and mice were killed at 9 a.m., 11 a.m., 3 p.m., 9 p.m., or 9 a.m. on the next day (24 h after ethanol administration) under fasting conditions. In studies of dose dependence, three different doses of ethanol (1, 3, and 5 g/kg body weight) were given to mice at 9 a.m., and mice were killed at 3 p.m. (6 h after ethanol administration).

2.3. Diet

To examine the effect of dietary fat on ethanol-induced fatty liver, mice were fed a fat-rich diet (30% of total energy, energy % [en%]) containing either safflower oil (high-oleic type) or fish oil. The fat diet was presented to mice at 6 p.m. on the day prior to ethanol administration. At 7 a.m. on the day of the study, food was removed from cages, and the mice were fasted. At 9 a.m., a solution of ethanol in water (40% v/v) at a dose of 3 g/kg body weight was administered intragastrically. As a control, a glucose solution (40% w/v) was administrated in a similar manner. Mice were killed at 3 p.m. (6 h after ethanol administration) under fasting conditions. A part of the liver was immediately homogenized with TRIzol Reagent (Invitrogen, Carlsbad, CA) and stored at −70 °C for isolation of RNA. Another part of the liver was frozen in liquid nitrogen and stored at −70 °C for TG assay. In experiment I, mice fed safflower oil or fish oil were compared. In experiment II, mice fed safflower oil or safflower oil plus Wy14643 (0.001% wt/wt) were compared. PPARα ligand Wy14643 was purchased from Cayman Chemicals (Ann Arbor, MI).

Diet preparations were similar to those of our previous studies (Table 1) [12,13]. Fatty-acid composition of dietary oils was measured by gas–liquid chromatography. Safflower oil (high-oleic type) contained 45% oleic acid (18:1n-9) and 46% linoleic acid (18:2n-6). Fish oil from tuna contained 7% eicosapentaenoic acid (20:5n-3) and 24% docosahexaenoic acid (22:6n-3). Fish oil was provided by NOF Corporation (Tokyo, Japan).

The mean food intake for 1 day was estimated by subtracting the food weight of that day from the initial food weight of the previous day and dividing this value by the number of mice housed in the cage. We were not able to measure food intake for individual mice because food was given in a common tray.

2.4. Other assays

Methods of RNA preparation, quantitative RT-PCR, liver lipid analysis, histologic analysis, and serum chemical analysis were described previously [14]. Primers used for quantitative RT-PCR were also described previously [14].

Table 1
Dietary composition of the fat diets (30 en%) in the present study

	Safflower oil (g/100 g)	Fish oil (g/100 g)
Safflower oil	13.0	–
Fish oil	–	13.0
Casein	29.0	29.0
Sucrose	7.3	7.3
α-Starch	36.5	36.5
Vitamin mix (AIN-93)	1.5	1.5
Mineral mix (AIN-93)	5.1	5.1
Cellulose powder	7.3	7.3
L-Cystine	0.4	0.4

2.5. Statistical analysis

Two-way analysis of variance (ANOVA) was used to examine the two main effects of dietary fat and ethanol and their interaction (SPSS for Windows, version 14.0, Tokyo, Japan). Statistical significance of the interaction of dietary fat and ethanol indicates that the effects of fish oil on ethanol differed statistically. When differences were significant with respect to main or interaction effects, each group was compared with the others by Student's t test. Statistical significance was set at $P < 0.05$. Values are shown as means ± SEM.

3. Results

3.1. Acute ethanol administration increases TG levels in liver

Mice were fed CE2 chow (normal laboratory diet) and then fasted for 2 h before ethanol administration. A single dose of ethanol (3 g/kg body weight) was given by gavage, and liver TG concentrations were monitored for 24 h in the fasting state (Fig. 1A). Glucose was administrated as a control. Mice exposed to ethanol showed 2-fold increases in liver TG concentrations at 2, 6, and 12 h after ethanol administration. However, because fasting alone gradually increased the TG concentration in liver, at 24 h after ethanol administration, there was no significant difference in the liver TG concentration between ethanol-treated mice and control mice. Expression of SREBP-1c mRNA was increased 2 h after ethanol administration but decreased gradually, and there was no difference at 12 h (Fig. 1B). In both groups of mice, the decrease in SREBP-1c mRNA expression in response to fasting was evident at 12 h after ethanol (or glucose) administration. An increase in expression of fatty-acid synthase (FAS) mRNA was followed by an increase in SREBP-1c mRNA; FAS mRNA was increased at 6 h after ethanol administration and then decreased (Fig. 1C). Because differences in TG accumulation and the FAS mRNA level between the two groups were largest at 6 h after ethanol administration, we killed mice 6 h after ethanol administration in the following experiments.

To examine the effect of the ethanol dose on the liver TG concentration, mice were given ethanol at 1, 3, or 5 g/kg body weight by gavage. A dose-dependent increase in the TG level in liver was observed (Fig. 2). However, when mice were given ethanol at 5 g/kg body weight, they became drowsy and fell asleep. To avoid the effects of sleeping, we used 3 g ethanol/kg body weight in the experiments described below.

3.2. Fish oil prevents ethanol-induced fatty liver

In experiment I, to examine the effect of fish oil in ethanol-induced fatty liver, mice were fed 30 en% fish oil on the day prior to ethanol administration. Control

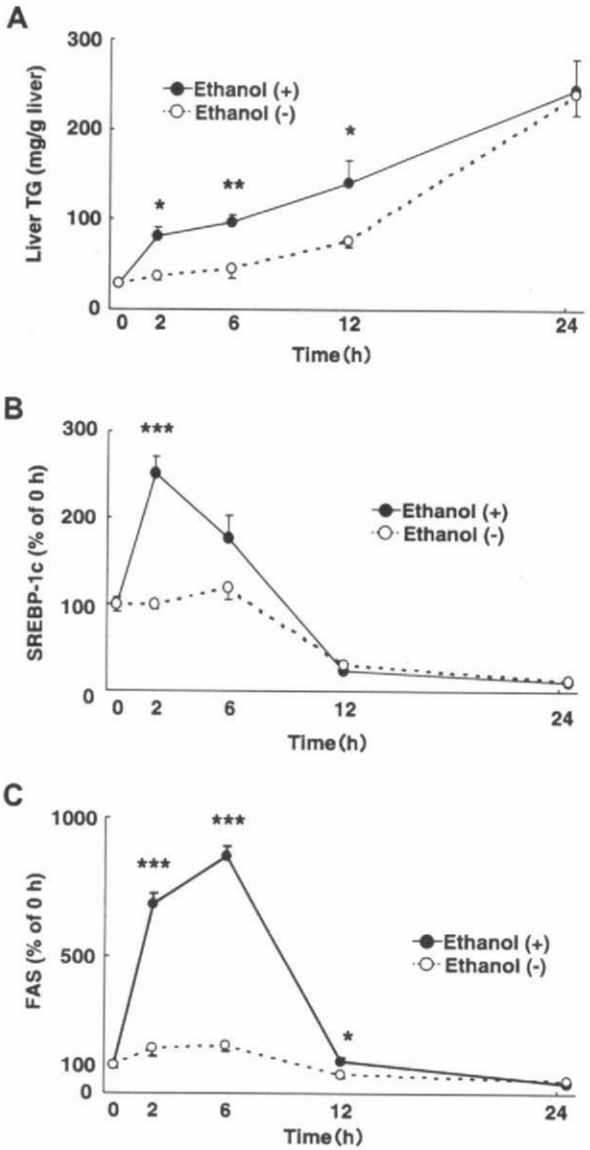

Fig. 1. Levels of triglyceride (TG) concentrations (A), SREBP1c mRNA (B), and FAS mRNA (C) over time in liver in response to acute ethanol administration. Mice fed CE2 on the day prior to ethanol administration were studied at various times after intragastric administration of ethanol (3 g/kg body weight) under fasting conditions. Values are means ± SEM (n = 8–12). $^{*}P < 0.05$, $^{**}P < 0.01$, $^{***}P < 0.001$ vs. no ethanol.

mice were fed 30 en% safflower oil. Liver weight of mice fed fish oil was 21% lower than that of mice fed safflower oil in the absence of ethanol (Table 2). However, this fish oil effect was not observed in the presence of ethanol; these results were reflected by a significant interaction of dietary fat and ethanol. The mechanisms of differential liver weights between each group of mice were not clear at the time. When mice were fed safflower oil, ethanol (3 g/kg body weight) significantly increased the TG concentrations in liver by 3.7-fold, whereas, when mice were fed fish oil, ethanol increased the TG

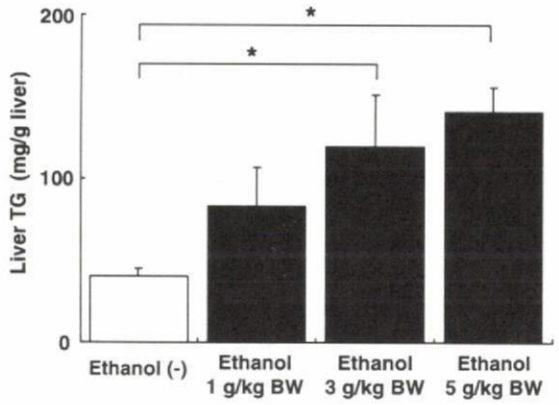

Fig. 2. Dose-dependent effect of ethanol on TG concentrations in liver. Mice fed CE2 on the day prior to ethanol administration were killed 6 h after intragastric administration of ethanol (1, 3, or 5 g/kg body weight) under fasting conditions. As a control, a glucose solutions [40% (w/v)] was given by gavage. Values are means ± SEM ($n = 4$). BW, body weight. *$P < 0.05$ vs. no ethanol.

concentration in liver by only 1.7-fold ($P = 0.857$) (Fig. 3A). The ethanol-induced increase in the liver TG concentration in mice fed fish oil was 73% less than that in mice fed safflower oil. A similar change in the whole-liver TG level was observed (Fig. 3B). Mice fed fish oil for 1 week showed a reduction in ethanol-induced fatty liver, similar to that observed in mice fed fish oil for 1 day (data not shown). Oil red O staining confirmed that TG accumulated in hepatocytes in mice fed safflower oil and that fish oil prevented ethanol-induced accumulation of TG in liver (Fig. 3C).

3.3. Effects of ethanol on mice fed safflower oil

The mechanism underlying development of ethanol-induced fatty liver in mice fed safflower oil was examined by expression profiling of hepatic genes. SREBP-1c is a major regulator of lipogenesis in the liver [5]. SREBP-1a is less abundant in the liver but is more potent in fatty acid synthesis than SREBP-1c [15]. To examine whether the increase in the hepatic TG level in response to ethanol was due to activation of SREBP-1, levels of mRNAs for SREBP-1 and the lipogenic enzymes FAS, stearoyl-CoA desaturase 1 (SCD1), and acetyl-CoA carboxylase 1 (ACC1) were determined by quantitative RT-PCR (Table 3). Ethanol increased expression of FAS and ACC1 mRNAs by 2- to 3-fold but did not affect levels of SREBP-1c, SREBP-1a, and SCD-1 mRNAs. However, ethanol increased expression of SREBP-1c mRNA by 1.6-fold in experiment II. The transcription factor liver X receptor (LXR) α binds to the SREBP-1c promoter and increases its expression [16]; however, ethanol did not affect LXRα mRNA expression. The coactivator peroxisome proliferator-activated receptor γ coactivator (PGC-1) β binds to

Table 2
Body and tissue weights, and serum analysis of mice on the experimental diets in experiment I

	Ethanol	Safflower oil	Fish oil	Two-way ANOVA P value		
				Fat	Ethanol	Fat × Ethanol
n	−	8	8			
	+	8	8			
Mean food intake (g/mouse)	−	4.9	3.9			
	+	5.2	3.9			
Weight (g)						
Body weight at start	−	22.7 ± 0.4	22.7 ± 0.3			
	+	22.6 ± 0.3	22.7 ± 0.3			
Final body weight	−	22.3 ± 0.4	21.5 ± 0.3	0.084	0.735	0.416
	+	21.9 ± 0.3	21.6 ± 0.2			
Liver	−	1.47 ± 0.08	1.16 ± 0.06[b]	<0.05	0.107	<0.05
	+	1.23 ± 0.07	1.19 ± 0.03			
n	−	8	7			
	+	8	8			
Serum analysis						
Glucose (mg/dL)	−	205 ± 25	196 ± 18	0.594	0.336	0.943
	+	187 ± 20	174 ± 18			
NEFA (mEq/L)	−	1.19 ± 0.11	1.32 ± 0.14	0.368	0.751	0.913
	+	1.24 ± 0.12	1.35 ± 0.16			
TG (mg/dL)	−	96 ± 26	119 ± 37	0.826	0.791	0.658
	+	121 ± 34	113 ± 42			
Insulin (ng/mL)	−	1.39 ± 0.20	0.50 ± 0.05[a]	<0.001	0.713	0.233
	+	1.24 ± 0.17	0.79 ± 0.21			

Values are means ± SEM.
[a] $P < 0.05$.
[b] $P < 0.01$ vs. safflower oil diet.

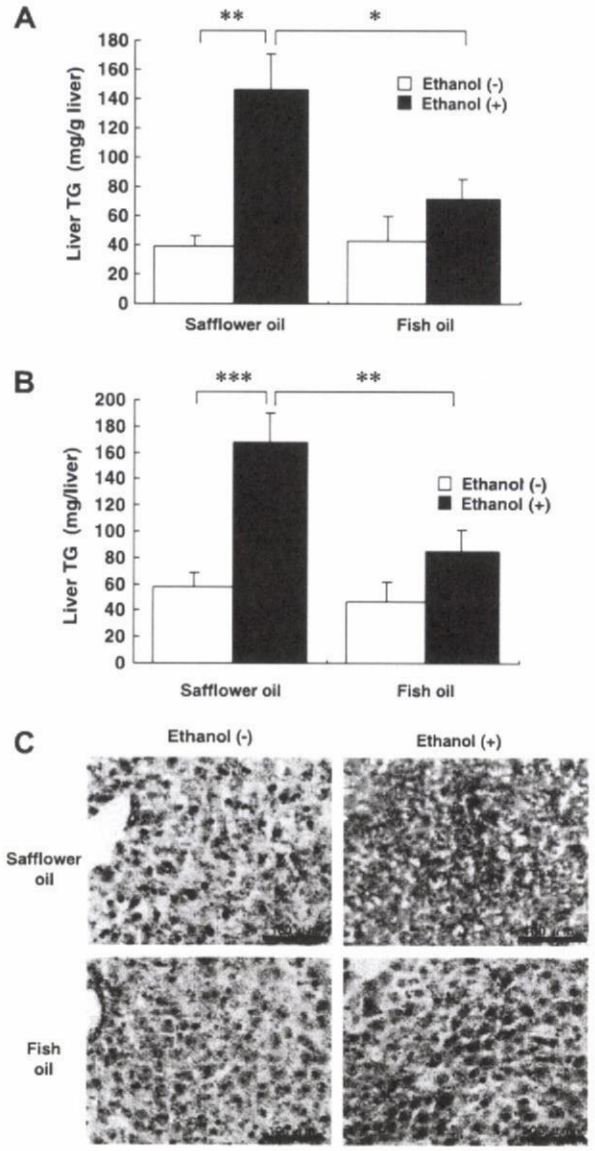

Fig. 3. Ingestion of fish oil on the day prior to ethanol administration prevents ethanol-induced fatty liver. Mice fed safflower oil-rich diet or fish oil-rich diet on the day prior to ethanol administration were killed 6 h after intragastric administration of ethanol (3 g/kg body weight) under fasting conditions. Hepatic lipids were extracted, and TG concentrations were measured (A). TG content in a whole liver of mouse (B). Values are means ± SEM ($n = 8$). $^{*}P < 0.05$, $^{**}P < 0.01$, $^{***}P < 0.001$. Oil red O staining of liver sections from mice (C). Original magnification 20×.

SREBP-1c and activates its transcriptional activity [17]; however, expression of PGC-1β mRNA was not altered in response to ethanol.

Acyl-CoA:diacylglycerol acyltransferase (DGAT) is responsible for the final esterification step of diacylglycerol to triacylglycerol [18], and Acyl-CoA:glycerol-3-phosphate acyltransferase (GPAT) is responsible for the first esterification step of glycerol-3-phosphate to monoacylglycerol [19]. These enzymes are involved in TG synthesis, and levels of DGAT1 and DGAT2 mRNAs were increased in response to ethanol.

Carbohydrate response element-binding protein (ChREBP) binds to and activates transcription of several lipogenic enzyme genes such as those for liver-type pyruvate kinase (LPK), a regulatory enzyme in the hepatic glycolysis pathway, ACC1, and FAS, leading to fatty liver [20]. Expression of ChREBP and LPK was increased in response to ethanol.

Activation of PPARγ causes fatty liver. Adenovirus-mediated delivery of PPARγ to hepatocytes leads to fatty liver [21], and PPARγ RNA interference is reported to decrease hepatic TG levels [22]. Therefore, we examined expression of PPARγ mRNA and its target, fatty-acid translocase (CD36). PPARγ consists of two forms, PPARγ1 and PPARγ2, and both forms are expressed in hepatocytes. Expression of mRNAs for both isoforms was increased in response to ethanol. However, expression of CD36 mRNA was not increased significantly. This might be due to inactivation of PPARα in response to ethanol; expression of CD36 mRNA is also increased by activation of PPARα [23].

Activation of PPARα and its target genes, including acyl-CoA oxidase (ACO, a marker of peroxisomal β-oxidation), medium-chain acyl-CoA dehydrogenase (MCAD, a marker of mitochondrial β-oxidation), and carnitine palmitoyltransferase 1 (CPT1, a marker of fatty-acid transport) increases fatty-acid β-oxidation [8]. Ethanol decreased the CPT1 mRNA level, but did not affect levels of other mRNAs. However, in experiment II, ethanol decreased expression of PPARα mRNA.

These data suggest that ethanol causes fatty liver through multiple mechanisms in mice fed safflower oil. Activation of transcription factors SREBP-1c and ChREBP promote fatty-acid synthesis, increases in PPARγ and DGATs mRNAs expression promote TG synthesis, and decreases in level of CPT1 mRNA lead to inhibition of fatty-acid oxidation. These changes were not specific to safflower oil. Similar gene expression profiles and development of fatty liver in response to ethanol were observed in mice fed saturated fat-rich butter (unpublished observation, S. Wada, T. Yamazaki, and O. Ezaki).

3.4. Effects of fish oil on expression of genes related to TG accumulation in liver

Fish oil feeding on the day prior to ethanol administration resulted in marked changes in gene expression in the absence of ethanol. Fish oil (30 en%) decreased expression of SREBP-1c and its target gene mRNAs (FAS, SCD1, and ACC1) and increased expression of PPARα and its target gene mRNAs (ACO, CPT1, and MCAD) (Table 3). Fish oil decreased the LPK mRNA level, suggesting that fish oil may also suppress ChREBP

Table 3
Hepatic gene expression profile of mice on the experimental diets in experiment I

	Ethanol	Safflower oil	Fish oil	Two-way ANOVA *P* value		
				Fat	Ethanol	Fat × Ethanol
n	–	8	8			
	+	8	8			
Gene expression						
Transcription factors related to lipogenesis						
SREBP-1c	–	100 ± 4	66 ± 7[b]	<0.001	0.493	0.113
	+	132 ± 24	54 ± 11[b]			
SREBP-1a	–	100 ± 2	79 ± 4[c]	<0.001	0.102	0.470
	+	90 ± 6	75 ± 5			
LXRα	–	100 ± 3	136 ± 6[c]	<0.001	0.630	0.769
	+	104 ± 5	167 ± 6[b]			
PGC-1β	–	100 ± 6	134 ± 16	0.553	0.961	0.127
	+	156 ± 67	81 ± 8			
Target genes of SREBP-1c						
FAS	–	100 ± 10	21 ± 1[c]	<0.001	<0.001	<0.05
	+	357 ± 33***	193 ± 17[c,***]			
SCD1	–	100 ± 6	37 ± 6[c]	<0.001	<0.05	0.371
	+	122 ± 7	47 ± 7[c]			
ACC1	–	100 ± 9	42 ± 2[c]	<0.001	<0.001	0.167
	+	345 ± 33***	235 ± 15[b,***]			
Enzymes related to TG synthesis						
DGAT1	–	100 ± 4	102 ± 5	0.728	<0.001	0.952
	+	132 ± 3***	134 ± 9**			
DGAT2	–	100 ± 5	115 ± 8	0.365	<0.001	0.416
	+	182 ± 12***	183 ± 10***			
GPAT	–	100 ± 7	92 ± 6	0.056	<0.05	0.173
	+	149 ± 22	107 ± 8			
ChREBP and target gene						
ChREBP	–	100 ± 5	106 ± 5	0.077	<0.001	0.246
	+	165 ± 13***	195 ± 12***			
LPK	–	100 ± 8	43 ± 5[c]	<0.001	<0.001	0.360
	+	211 ± 11***	171 ± 12[a,***]			
PPARγ and target genes						
PPARγ1	–	100 ± 11	121 ± 12	0.745	<0.001	0.355
	+	197 ± 23**	187 ± 18**			
PPARγ2	–	100 ± 30	126 ± 47	0.203	<0.05	0.146
	+	775 ± 248*	395 ± 95*			
CD36	–	100 ± 7	167 ± 23	0.195	0.205	0.183
	+	167 ± 22	166 ± 38			
PPARα and target genes						
PPARα	–	100 ± 1	186 ± 18[c]	<0.001	<0.01	<0.01
	+	83 ± 12	102 ± 15**			
MCAD	–	100 ± 3	308 ± 37[c]	<0.001	0.706	0.078
	+	154 ± 14	272 ± 29[b]			
ACO	–	100 ± 8	350 ± 35[c]	<0.001	<0.05	<0.01
	+	121 ± 12	226 ± 22[c,**]			
CPTI	–	100 ± 3	147 ± 20[a]	<0.05	<0.05	0.633
	+	73 ± 9*	105 ± 23			

Values are means ± SEM.
[a] $P < 0.05$.
[b] $P < 0.01$.
[c] $P < 0.001$ vs. safflower oil diet.
* $P < 0.05$.
** $P < 0.01$.
*** $P < 0.001$ vs. no ethanol.

activity. Although changes in expression of these genes favored reduction in the liver TG concentration, the liver TG level was not lower in mice fed fish oil than in mice fed safflower oil (**Fig. 3**), suggesting that SREBP-1c and ChREBP activity may not be involved in regulating the basal liver TG concentration. Fish oil

Table 4
Body and tissue weights, liver TG and gene expression profiles of mice on the experimental diets in experiment II

	Ethanol	Safflower oil	Safflower oil + Wy14643	Two-way ANOVA *P* value		
				Wy14643	Ethanol	Wy × Ethanol
n	−	8	8			
	+	8	8			
Mean food intake (g/mouse)	−	4.4	3.7			
	+	4.2	3.9			
Weight (g)						
Final body weight	−	23.2 ± 0.3	22.8 ± 0.2	0.161	0.979	0.587
	+	23.1 ± 0.2	22.9 ± 0.2			
Liver	−	1.45 ± 0.05	1.26 ± 0.02[b]	<0.01	0.052	0.072
	+	1.31 ± 0.05	1.25 ± 0.03			
Liver TG (mg/g liver)	−	32 ± 2	35 ±2	0.134	<0.001	0.272
	+	104 ± 6***	121 ± 12***			
Gene expression						
Transcription factors related to lipogenesis						
SREBP-1c	−	100 ± 7	100 ± 7	<0.01	<0.05	<0.01
	+	156 ± 11***	89 ± 11[c]			
SREBP-1a	−	100 ± 3	92 ± 3	<0.01	0.422	0.218
	+	109 ± 5	91 ± 5[a]			
LXRα	−	100 ± 3	114 ± 4[a]	<0.001	<0.05	0.913
	+	93 ± 2	107 ± 3[b]			
PGC-1β	−	100 ± 5	96 ± 3	0.528	<0.01	0.979
	+	81 ± 6*	77 ± 9			
Target genes of SREBP-1c						
FAS	−	100 ± 10	42 ± 5[c]	<0.001	<0.001	0.084
	+	352 ± 36***	205 ± 31[b,***]			
SCD1	−	100 ± 5	95 ± 4	0.745	<0.05	0.491
	+	107 ± 7	109 ± 6*			
ACC1	−	100 ± 9	63 ± 6[b]	<0.001	<0.001	<0.01
	+	390 ± 45***	199 ± 28[b,***]			
Enzymes related to TG synthesis						
DGAT1	−	100 ± 2	90 ± 3	0.672	<0.001	0.268
	+	126 ± 11*	130 ± 5***			
DGAT2	−	100 ± 2	106 ± 4	<0.01	<0.001	<0.001
	+	175 ± 4***	148 ± 4[c,***]			
GPAT	−	100 ± 8	116 ± 6	0.292	0.076	0.296
	+	94 ± 8	94 ± 7			
ChREBP and target gene						
ChREBP	−	100 ± 2	100 ± 2	<0.01	<0.001	<0.01
	+	205 ± 11***	156 ± 8[b,***]			
LPK	−	100 ± 7	25 ± 2[c]	<0.001	<0.001	<0.01
	+	246 ± 19***	98 ± 13[c,***]			
PPARγ and target genes						
PPARγ1	−	100 ± 4	156 ± 5[c]	<0.001	<0.001	0.051
	+	163 ± 10***	186 ± 10*			
PPARγ2	−	100 ± 12	76 ± 8	<0.05	<0.001	0.076
	+	403 ± 76**	214 ± 45**			
CD36	−	100 ± 4	640 ± 35[c]	<0.001	0.429	0.689
	+	113 ± 14	679 ± 52[c]			
PPARα and target genes						
PPARα	−	100 ± 4	169 ± 11[c]	<0.001	<0.001	0.990
	+	54 ± 5***	122 ± 11[c,*]			
MCAD	−	100 ± 4	381 ± 24[c]	<0.001	0.607	0.054
	+	122 ± 7	343 ± 15[c]			
ACO	−	100 ± 2	489 ± 17[c]	<0.001	0.142	0.218
	+	97 ± 5	456 ± 16[c]			
CPTI	−	100 ± 3	188 ± 14[c]	<0.001	<0.01	0.642
	+	61 ± 4***	159 ± 12[c]			

Values are means ± SEM.
[a] $P < 0.05$.
[b] $P < 0.01$.
[c] $P < 0.001$ vs. safflower oil diet.
* $P < 0.05$.
** $P < 0.01$.
*** $P < 0.001$ vs. no ethanol.

did not affect expression of genes related to TG synthesis (DGAT1, DGAT2, and GPAT) or PPARγ-related genes (PPARγ1, PPARγ2, and CD36).

3.5. Effects of ethanol administration on mice fed fish oil

Fish oil decreased basal (without ethanol) SREBP-1c mRNA and expression of its target genes; however, ethanol itself did not impair its ability to induce expression of these genes. In mice fed safflower oil, ethanol increased expression of FAS, SCD1, and ACC1 mRNAs by 3.6-, 1.2-, and 3.5-fold, respectively, whereas in mice fed fish oil, ethanol increased expression of these genes by 9.2-, 1.3-, and 5.6-fold, respectively (Table 3). As a result, FAS and ACC1 mRNA levels in ethanol-treated mice fed fish oil were 1.9- and 2.4-fold higher, respectively, than levels in mice fed safflower oil without ethanol. The mean SCD1 mRNA level in ethanol-treated mice fed fish oil was 53% lower than that in mice fed safflower oil without ethanol. Increased expression of DGAT1, DGAT2, ChREBP, LPK, and PPARγ mRNAs in response to ethanol was observed in mice fed fish oil and in mice fed safflower oil.

Ethanol decreased fish oil-induced activation of PPARα. Ethanol decreased expression of PPARα and ACO mRNAs by 45% and 35%, respectively, in mice fed fish oil. However, MCAD and ACO mRNA levels in ethanol-treated mice fed fish oil were still higher than those in mice fed safflower oil without ethanol.

3.6. Serum nonesterified fatty acid (NEFA), TG, and glucose concentrations do not differ between groups

Increased plasma concentrations of glucose and NEFA may promote hepatic steatosis [24]. Insulin upregulates SREBP-1c expression [25]. We measured serum glucose, NEFA, TG, and insulin concentrations at 3 and 6 h after ethanol administration (only the 6-h data are shown in Table 2). There were no significant differences in glucose, NEFA, and TG concentrations between the groups, suggesting that substrate entry (NEFA, glucose) into and exit (TG) from the liver were not altered markedly and that lipolysis in adipose tissue might not be enhanced after ethanol administration under this condition. The serum insulin concentration in mice fed fish oil was slightly lower than that in mice fed safflower oil, suggesting that a decrease in SREBP-1c in mice fed fish oil was due, at least in part, to a decrease in the insulin concentration.

3.7. Wy14643 does not affect ethanol-induced fatty liver

Although ethanol inhibited activation of PPARα, fish oil-fed mice still showed increased PPARα activity even after ethanol administration. In experiment II, to examine the role of PPARα activation in the fish oil-mediated prevention of ethanol-induced fatty liver, a PPARα activator, Wy14643, was given with safflower oil on the day prior to ethanol administration, and then the effect of ethanol was investigated. A dose of 0.001% (wt/wt) Wy14643 was chosen because at this dose, the increases in expression of PPARα, ACO, CPT1, and MCAD mRNAs were similar to the increases observed in mice fed 30 en% fish oil. Although marked increases in expression of these genes, which promote fatty-acid oxidation, were observed in Wy14643-administrated mice with or without ethanol, Wy14643 supplementation did not prevent ethanol-induced fatty liver (Table 4). A higher dose of Wy14643 (0.1%) also failed to prevent ethanol-induced fatty liver (data not shown). Wy14643 affected expression of other genes. With or without ethanol, Wy14643 decreased expression of FAS, ACC1, and LPK mRNAs and increased expression of PPARγ1 and CD36 mRNAs. A marked increase in CD36 mRNA was observed in mice treated with Wy14643, but this alteration was not observed in mice fed fish oil.

4. Discussion

Administration of a single dose of ethanol to mice causes fatty liver. Ethanol-induced fatty liver was observed in mice fed CE2 (high-carbohydrate, normal laboratory diet) or a safflower oil-rich diet. There are multiple mechanisms underlying ethanol-induced development of fatty liver (Fig. 4). Ethanol administration activates SREBP-1c and ChREBP, which promote *de novo* fatty-acid synthesis; increases expression of mRNAs encoding PPARγ and DGATs, which promote TG synthesis; and decreases expression of mRNA encoding in CPT1, which leads to inhibition of fatty-acid oxidation.

Ingestion of fish oil on the day prior to ethanol treatment reduced ethanol-induced fatty liver by 73% (experiment I), whereas a PPARα activator, Wy14643, did not prevent ethanol-induced fatty liver (experiment II). Differences in gene expression profiles between the two experiments suggest that decreases in expression of lipogenic genes in response to Wy14643 are not sufficient to prevent ethanol-induced fatty liver. Reduction of SCD1 was not observed in mice supplemented with Wy14634, and an increase in CD36 mRNA in response to Wy14643 may also promote fatty liver (Table 4 and Fig. 4). Liver-specific SCD1-knockout mice are protected from hepatic steatosis induced by a high-carbohydrate diet [26], and an increased CD36 level in liver promotes fatty liver [27]. The mechanisms that underlie the decreases in FAS and ACC1 mRNAs in response to Wy14643 are not clear at present. The portion of ethanol-induced fatty liver not inhibited by fish oil may develop due to remaining increased expression of FAS, ACC1, and LPK, which promote *de novo* fatty-acid syn-

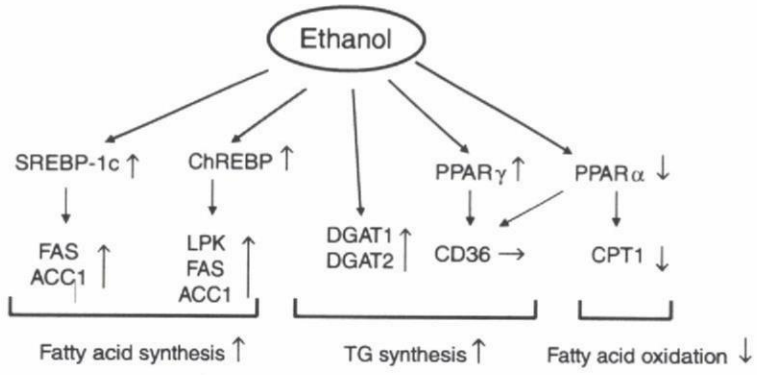

Fig. 4. Mechanisms of ethanol-induced fatty liver. There are multiple mechanisms underlying ethanol-induced development of fatty liver. Ethanol administration activates SREBP-1c and ChREBP, which promote *de novo* fatty-acid synthesis. This increases expression of mRNAs encoding of PPARγ and DGATs, which promote TG synthesis. It deactivates PPARα leading to a decrease in the expression of mRNA encoding in CPT1, which in turn inhibition of fatty-acid oxidation. CD36 mRNA remains unchanged, due to the balance of activation of PPARγ and deactivation of PPARα (activation of either PPARγ or PPARα leads to increase CD36 mRNA). Prior ingestion of fish oil effectively prevents ethanol-induced fatty liver. This reduction is at least in part due to a decrease in basal SREBP-1c activity and largely a result of the reduction in SCD1. Prior administration of Wy14643, PPARα activator, did not inhibit ethanol-induced fatty liver because of an unchanged expression in SCD1 and a marked increase in CD36.

thesis, and/or the increased TG synthesis from fatty acids, as was suggested by increases in PPARγ and DGATs mRNAs.

Patients with liver damage were shown to have a lower 20:4/18:0 ratio than patients without liver damage [28]. Rhesus monkeys maintained on a diet low in linoleate and linolenate developed liver fibrosis after consuming alcohol over a period of 3 years [29]. Consistent with our present observations, these data indicate that substantial intake of polyunsaturated fatty acids may be favorable for prevention of ethanol-induced fatty liver. Although 30 en% fish oil was used in the present study to examine the mechanisms, a lower dose of fish oil also prevented ethanol-induced fatty liver. Mice fed 10 en% fish oil on the day prior to ethanol administration showed a 37% lower TG concentration in liver than mice without fish oil (unpublished observation, S. Wada, T. Yamazaki, and O. Ezaki). The 10 en% fish oil is comparable to the level consumed by humans [30].

The present findings indicate that habitual intake of fish oil may prevent development of fatty liver in response to ethanol consumption.

Acknowledgements

This work was supported in part by a grant-in-aid for scientific research Kakenhi from the Japanese Ministry of Education, Culture, Sports, Science and Technology (MEXT, Tokyo, Japan); by research grants from the Japanese Ministry of Health, Labour, and Welfare; by a grant-in-aid for the Development of Evaluation and Management Methods for Supply of Safe, Reliable, and Functional Food and Farm Produce from the Japanese Ministry of Agriculture, Forestry and Fisheries; and by a grant for the Promotion of Fundamental Studies in Health Sciences from the Organization for Pharmaceutical Safety and Research (OPSR, Osaka, Japan).

References

[1] Purohit V, Russo D, Coates PM. Role of fatty liver, dietary fatty acid supplements, and obesity in the progression of alcoholic liver disease: introduction and summary of the symposium. Alcohol 2004;34:3–8.
[2] Carson EJ, Pruett SB. Development and characterization of a binge drinking model in mice for evaluation of the immunological effects of ethanol. Alcohol Clin Exp Res 1996;20:132–138.
[3] Lieber CS, DeCarli LM, Schmid R. Effect of ethanol on fatty acid metabolism in liver slices. Biochem Biophys Res Commun 1959;1:302–306.
[4] Horning MG, Williams EA, Maling HM, Brodie BB. Depot fat as source of increased liver triglycerides after ethanol. Biochem Biophys Res Commun 1960;3:635–640.
[5] Horton JD, Shimomura I. Sterol regulatory element-binding proteins: activators of cholesterol and fatty acid biosynthesis. Curr Opin Lipidol 1999;10:143–150.
[6] You M, Fischer M, Deeg MA, Crabb DW. Ethanol induces fatty acid synthesis pathways by activation of sterol regulatory element-binding protein (SREBP). J Biol Chem 2002;277:29342–29347.

[7] Ji C, Chan C, Kaplowitz N. Predominant role of sterol response element binding proteins (SREBP) lipogenic pathways in hepatic steatosis in the murine intragastric ethanol feeding model. J Hepatol 2006;45:717–724.
[8] Reddy JK, Mannaerts GP. Peroxisomal lipid metabolism. Annu Rev Nutr 1994;14:343–370.
[9] Galli A, Pinaire J, Fischer M, Dorris R, Crabb DW. The transcriptional and DNA binding activity of peroxisome proliferator-activated receptor alpha is inhibited by ethanol metabolism. A novel mechanism for the development of ethanol-induced fatty liver. J Biol Chem 2001;276:68–75.
[10] Fischer M, You M, Matsumoto M, Crabb DW. Peroxisome proliferator-activated receptor alpha (PPARalpha) agonist treatment reverses PPARalpha dysfunction and abnormalities in hepatic lipid metabolism in ethanol-fed mice. J Biol Chem 2003;278:27997–28004.
[11] Capanni M, Calella F, Biagini MR, Genise S, Raimondi L, Bedogni G, et al. Prolonged n-3 polyunsaturated fatty acid supplementation ameliorates hepatic steatosis in patients with non-alcoholic fatty liver disease: a pilot study. Aliment Pharmacol Ther 2006;23:1143–1151.
[12] Kim HJ, Takahashi M, Ezaki O. Fish oil feeding decreases mature sterol regulatory element-binding protein 1 (SREBP-1) by down-regulation of SREBP-1c mRNA in mouse liver. A possible mechanism for down-regulation of lipogenic enzyme mRNAs. J Biol Chem 1999;274:25892–25898.
[13] Nakatani T, Kim HJ, Kaburagi Y, Yasuda K, Ezaki O. A low fish oil inhibits SREBP-1 proteolytic cascade, while a high-fish-oil feeding decreases SREBP-1 mRNA in mice liver: relationship to anti-obesity. J Lipid Res 2003;44:369–379.
[14] Yamazaki T, Nakamori A, Sasaki E, Wada S, Ezaki O. Fish oil prevents sucrose-induced fatty liver but exacerbates high-safflower oil-induced fatty liver in ddY mice. Hepatology 2007;46:1779–1790.
[15] Shimano H, Horton JD, Hammer RE, Shimomura I, Brown MS, Goldstein JL. Overproduction of cholesterol and fatty acids causes massive liver enlargement in transgenic mice expressing truncated SREBP-1a. J Clin Invest 1996;98:1575–1584.
[16] Repa JJ, Liang G, Ou J, Bashmakov Y, Lobaccaro JM, Shimomura I, et al. Regulation of mouse sterol regulatory element-binding protein-1c gene (SREBP-1c) by oxysterol receptors, LXRα and LXRβ. Genes Dev 2000;14:2819–2830.
[17] Lin J, Yang R, Tarr PT, Wu PH, Handschin C, Li S, et al. Hyperlipidemic effects of dietary saturated fats mediated through PGC-1β coactivation of SREBP. Cell 2005;120:261–273.
[18] Yamazaki T, Sasaki E, Kakinuma C, Yano T, Miura S, Ezaki O. Increased very low density lipoprotein secretion and gonadal fat mass in mice overexpressing liver DGAT1. J Biol Chem 2005;280:21506–21514.
[19] Thuresson ER. Inhibition of glycerol-3-phosphate acyltransferase as a potential treatment for insulin resistance and type 2 diabetes. Curr Opin Invest Drugs 2004;5:411–418.
[20] Uyeda K, Yamashita H, Kawaguchi T. Carbohydrate responsive element-binding protein (ChREBP): a key regulator of glucose metabolism and fat storage. Biochem Pharmacol 2002;63:2075–2080.
[21] Yu S, Matsusue K, Kashireddy P, Cao WQ, Yeldandi V, Yeldandi AV, et al. Adipocyte-specific gene expression and adipogenic steatosis in the mouse liver due to peroxisome proliferator-activated receptor γ1 (PPARγ1) overexpression. J Biol Chem 2003;278:498–505.
[22] Herzig S, Hedrick S, Morantte I, Koo SH, Galimi F, Montminy M. CREB controls hepatic lipid metabolism through nuclear hormone receptor PPAR-γ. Nature 2003;426:190–193.
[23] Guerre-Millo M, Gervois P, Raspe E, Madsen L, Poulain P, Derudas B, et al. Peroxisome proliferator-activated receptor α activators improve insulin sensitivity and reduce adiposity. J Biol Chem 2000;275:16638–16642.
[24] Chitturi S, Abeygunasekera S, Farrell GC, Holmes-Walker J, Hui JM, Fung C, et al. NASH and insulin resistance: Insulin hypersecretion and specific association with the insulin resistance syndrome. Hepatology 2002;35:373–379.
[25] Shimomura I, Bashmakov Y, Ikemoto S, Horton JD, Brown MS, Goldstein JL. Insulin selectively increases SREBP-1c mRNA in the livers of rats with streptozotocin-induced diabetes. Proc Natl Acad Sci USA 1999;96:13656–13661.
[26] Miyazaki M, Flowers MT, Sampath H, Chu K, Otzelberger C, Liu X, et al. Hepatic stearoyl-CoA desaturase-1 deficiency protects mice from carbohydrate-induced adiposity and hepatic steatosis. Cell Metab 2007;6:484–496.
[27] Koonen DP, Jacobs RL, Febbraio M, Young ME, Soltys CL, Ong H, et al. Increased hepatic CD36 expression contributes to dyslipidemia associated with diet-induced obesity. Diabetes 2007;56:2863–2871.
[28] de la Maza MP, Hirsch S, Nieto S, Petermann M, Bunout D. Fatty acid composition of liver total lipids in alcoholic patients with and without liver damage. Alcohol Clin Exp Res 1996;20:1418–1422.
[29] Pawlosky RJ, Flynn BM, Salem Jr N. The effects of low dietary levels of polyunsaturates on alcohol-induced liver disease in rhesus monkeys. Hepatology 1997;26:1386–1392.
[30] Feskens EJ, Kromhout D. Epidemiologic studies on Eskimos and fish intake. Ann NY Acad Sci 1993;683:9–15.

BRAIN RESEARCH REVIEWS 57 (2008) 363–375

available at www.sciencedirect.com

ScienceDirect

www.elsevier.com/locate/brainresrev

BRAIN RESEARCH REVIEWS

Review

Rapid modulation of synaptic plasticity by estrogens as well as endocrine disrupters in hippocampal neurons

Mari Ogiue-Ikeda[a,b,c,1], *Nobuaki Tanabe*[a,b,1], *Hideo Mukai*[a,b,d], *Yasushi Hojo*[a,b,d], *Gen Murakami*[a,d], *Tomokazu Tsurugizawa*[a,b], *Norio Takata*[a,c], *Tetsuya Kimoto*[a,b], *Suguru Kawato*[a,b,c,d,*]

[a]*Department of Biophysics and Life Sciences, Graduate School of Arts and Sciences, The University of Tokyo, 3-8-1 Komaba, Meguro, Tokyo 153-8902, Japan*

[b]*Core Research for Evolutional Science and Technology Project of Japan Science and Technology Agency, The University of Tokyo, Japan*

[c]*Project of Special Coordinate Funds for Promoting Science and Technology, The University of Tokyo, Japan*

[d]*Bioinformatics Project of Japan Science and Technology Agency, The University of Tokyo, Japan*

ARTICLE INFO

Article history:
Accepted 1 June 2007
Available online 28 July 2007

Keywords:
Hippocampus
Estradiol
Endocrine disrupter
Estrogen receptor
Synaptic plasticity
Bisphenol A

ABSTRACT

Estrogen modulates memory-related synaptic plasticity not only slowly but also rapidly in the hippocampus. However, molecular mechanisms of the rapid action are yet largely unknown. We here describe rapid modulation of representative synaptic plasticity, i.e., long-term depression (LTD), long-term potentiation (LTP) and spinogenesis, by 17beta-estradiol, selective estrogen agonists as well as endocrine disrupters.

The authors demonstrated that 1–10 nM estradiol induced rapid enhancement of LTD within 1 h in not only CA1 but also CA3 and dentate gyrus (DG). On the other hand, the modulation of LTP by estradiol was not statistically significant.

The total density of spines was increased in CA1 pyramidal neurons, within 2 h after application of estradiol. The total density of thorns (postsynaptic spine-like structure) was, however, decreased by estradiol in CA3 pyramidal neurons. Both the increase of spines in CA1 and the decrease of thorns in CA3 were completely suppressed by Erk MAP kinase inhibitor. Only ERalpha agonist PPT induced the same enhancement/suppression effect as estradiol on both LTD and spinogenesis in CA1 and CA3. ERbeta agonist DPN induced completely different results.

ERalpha localized in spines and presynapses of principal glutamatergic neurons in CA1, CA3 and DG. The same ERalpha was also located in nuclei and cytoplasm. Identification of ERalpha was successfully performed using purified RC-19 antibody. Non-purified ERalpha antisera, however, reacted significantly with unknown proteins, resulting in wrong immunostaining different from real ERalpha distribution.

An issue of 'endocrine disrupters' (1–100 nM low dose of environmental chemicals), which are artificial xenoestrogenic or anti-xenoestrogenic substances, has emerged as a

* *Corresponding author.* Department of Biophysics and Life Sciences, Graduate School of Arts and Sciences, The University of Tokyo, 3-8-1 Komaba, Meguro, Tokyo 153-8902, Japan. Fax: +81 3 5454 6517.
E-mail address: kawato@phys.c.u-tokyo.ac.jp (S. Kawato).

Abbreviations: BPA, bisphenol A; CNQX, cyano-nitroquinoxaline-dione; DES, diethylstilbestrol; DPN, diarylpropionitrile; LTD, long-term depression; LTP, long-term potentiation; NMDA, N-methyl-D-aspartate; NP, 4-nonylphenol; PPT, propyl-pyrazole-trinyl-pheno

[1] Contributed equally to the present work.

0165-0173/$ – see front matter
doi:10.1016/j.brainresrev.2007.06.010

social and environmental problem. Endocrine disrupters were found to significantly modulate LTD and spinogenesis. Bisphenol A (BPA) and diethylstilbestrol (DES) enhanced LTD in CA1 and CA3. The total spine density was significantly increased by BPA and DES in CA1. Most probable receptors for BPA and DES may be Ralpha; however, other receptors might also be involved.

Contents

1. Introduction

Estradiol exerts rapid (e.g., 1 h) influence on the synaptic plasticity of rat hippocampal glutamatergic neurons in slices, as has been demonstrated by a number of electrophysiological investigations in rats and mice, concerning the long-term potentiation (LTP) in CA1 (Balthazart and Ball, 2000; Foy et al., 1999), the long-term depression (LTD) in CA1 (Vouimba et al., 2000) or kainate current in CA1 (Gu and Moss, 1996; Gu et al., 1999). To explain this modulation, attempts have been made to identify synaptic/membrane estrogen receptors in the hipocampus (Mukai et al., 2007). On the other hand, extensive studies have been performed to investigate the role of estrogens in slowly (1–4 days) modulating hippocampal plasticity, because the hippocampus is known to be a target for the actions of gonadal estrogens reaching the brain via the circulation. For example, the density of dendritic spines in the CA1 pyramidal neurons is modulated *in vivo* by estrogen replacement in ovariectomized animals (Gould et al., 1990; MacLusky et al., 2005; Woolley et al., 1990; Woolley and McEwen, 1992) and androgens in castrated animals (MacLusky et al., 2005), resulting in increase/recovery of the number of spines and spine-synapses.

The site of estrogen action in the hippocampus is a matter of debate for more than a decade. So far, two distinct types of estrogen receptor have been identified in the mammalian brain: ERα (McEwen, 2002; Simerly et al., 1990) and ERβ (Mitra et al., 2003; Shughrue et al., 1997). The rapid effect of estrogen may be achieved by either ERα or ERβ possibly localized at the membrane, in analogy with cultured cells of peripheral origin (McEwen and Alves, 1999; Razandi et al., 1999). Subcellular and cellular localization of estrogen receptors is still not fully elucidated even for ERα, particularly in adult rat hippocampus. Many studies have reported in female rats that ERα immunoreactivity has been found in the nuclei of scattered inhibitory gamma-aminobutyric acid (GABA)ergic interneurons by light or electron microscopy using AS409 antiserum against ERα (Milner et al., 2001; Orikasa et al., 2000; Woolley et al., 1997). It is therefore assumed that interneurons are the targets of estrogen action.

In contrast, we have been exploring the possibility that estrogen may exert its effects directly on principal neurons, because of growing evidence such as an NMDA receptor-dependent mechanism of estradiol regulation on dendritic spine density (Woolley and McEwen, 1994), and increase of glutamate binding to NMDA receptors by estradiol (Woolley et al., 1997). Recently, we successfully demonstrated that 17β-estradiol enhanced the long-term depression (LTD) as well as new spinogenesis within 1–2 h estradiol treatments of the adult rat hippocampus (Ishii et al., 2006). We also successfully determined the synaptic localization of ERα which may predominantly catalyze these modulations. In considering the role of estrogen in memory processing, its effect on LTD is essential. LTD is not simply a "forgetting" mechanism, but LTD may be a positive mechanism used to "correct" wrong memories formed by initial LTP processes which store not only correct information but also wrong information (Migaud et al., 1998). Regulation of spinogenesis is another important role of estrogen in memory processes due to serving new spines for creating new synapses.

Because the memory-related synaptic plasticity is modulated by estradiol, it is reasonable to postulate that orally administered estrogen-like endocrine disrupters (i.e., low dose of environmental chemicals) might also affect synaptic plasticity (Kawato, 2004), when reaching neurons via the blood circulation and by crossing the blood–brain barrier. Bisphenol A (BPA) is suspected to disturb estrogen functions in the brain tissues, since BPA has been shown to reach the brain of both mother and fetus within 1 h after s.c. injection to mother rat (Uchida et al., 2002). The time required for BPA to reach the brain was not significantly different from that required to reach other peripheral organs. In contrast to the efficient detoxification of endocrine disrupters in the liver, detoxification in the brain may be much less efficient, due to the extremely low level of drug-metabolizing enzymes (e.g., cytochrome P450s) in the brain (Chinta et al., 2005; Hojo et al., 2004; Kishimoto et al., 2004; Miksys and Tyndale, 2002). These findings suggest that endocrine disrupters actually reach mammalian brains (including human brains) and then disrupt their functions. We here demonstrate the rapid effects of 10–100 nM endocrine disrupters such as bisphenol A (BPA),

diethylstilbestrol (DES) and 4-nonylphenol (NP) on LTD and spinogenesis.

2. Rapid modulation of synaptic plasticity by estrogens

2.1. *LTD and LTP*

17β-Estradiol may rapidly modulate two different types of synaptic plasticity of neurons. One is synaptic transmission such as LTD or LTP, and the other is spinogenesis. LTD and LTP probe the characteristics of preformed synapses, whereas spinogenesis analyzes not only spine-synapses (spines forming synapses) but also free spines (spines without forming synapses). Estradiol-induced modulation of LTD or LTP occurs only in preexistent synapses, because newly generated spines by estradiol treatments do not form new synapses within 2 h, as judged from no increase in the baseline magnitude of EPSP signal during 2 h of estradiol perfusion (Mukai et al., 2007).

Evidence is emerging that estradiol exerts a rapid influence (0.5–1 h) on synaptic transmission of hippocampal slices from adult rats, as demonstrated by electrophysiology (Foy et al., 1999; Gu and Moss, 1996; Ito et al., 1999; Shibuya et al., 2003; Teyler et al., 1980). In case of the occasionally observed enhancement of LTP by 1–10 nM estradiol in CA1 pyramidal neurons, a baseline increase by 20–30% has always been observed upon the onset of 10 nM estradiol perfusion in the initial slope of the excitatory postsynaptic potential (EPSP), which has been attendant upon a further increase to approximately 160% upon high-frequency tetanic stimulation of Schaffer collaterals of hippocampus from adult rat (3 months) (Fig. 1) (Bi et al., 2000; Foy et al., 1999; Kawato, 2004). However, without this 20–30% baseline increase in EPSP slope (before the tetanic stimulation), the enhancement of LTP by estradiol is not apparent, with regard to the pure tetanic stimulation-induced LTP. In other words, the magnitude of pure tetanic stimulation-induced LTP (approximately 130%) is nearly the same between the presence and the absence of 10 nM estradiol (Fig. 1) (Ito et al., 1999; Kawato, 2004). It should be noted that in 3–4 weeks rats, 10 nM estradiol even suppressed LTP-induction down to the same level as that for adult rats (Ito et al., 1999; Shibuya et al., 2003). Estradiol effects on LTP seem to be significantly dependent on the age of rats.

In memory processing, not only LTP (memory forming mechanism) but also LTD is essential. Mutant mice, which show enhanced LTP and suppressed LTD, have shown impaired learning of Morris water maze (Migaud et al., 1998). This suggests that LTD may be required to "correct" wrong memories formed by initial LTP processes which store not only correct information but also wrong information.

We found that LTD was very sensitive to 17β-estradiol treatments in hippocampal slices from adult male rats. We demonstrated, for the first time, a significant rapid enhancement of LTD by 1–10 nM estradiol perfusion in CA1, CA3 and dentate gyrus (DG) (Fig. 2) (Mukai et al., 2007). Recordings were performed using 64 planar multielectrodes particularly arranged to stimulate the Schaffer collaterals in the stratum radiatum of CA1, the recurrent collateral fibers in the stratum radiatum of CA3, and the medial perforant pathways in the molecular layer of DG. LTD was induced pharmacologically by

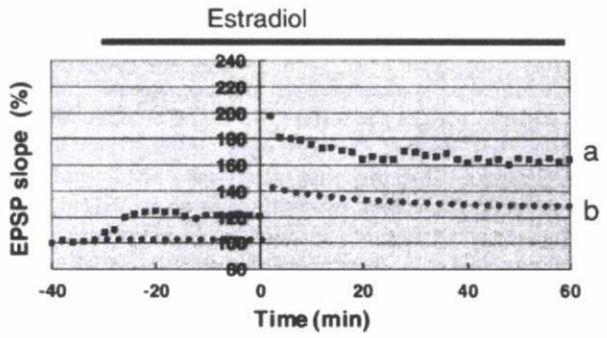

Fig. 1 – Rapid modulation of LTP by 17β-estradiol in CA1 of hippocampal slices from adult male rats. In some slices such as curve a (blue square, $n=5$) (observed for less than 5 slices out of 100 slices), preperfusion of 10 nM estradiol for 30 min at 30 °C increased the baseline slope of the excitatory postsynaptic potential (EPSP) to approximately 120–130%. Upon tetanic stimulation (100 Hz, 1 s, at $t=0$) of the Schaffer collaterals, EPSP slope was significantly increased to the final level of 164.4±12.6% (LTP-induction). In many slices such as curve b (red circle, $n=6$), when an increase in the baseline EPSP slope did not occur by perfusion of 10 nM estradiol (observed for nearly 95 slices out of 100 slices), EPSP slope was increased to 132.1±7.8% upon tetanic stimulation. The difference between curves a and b is primarily due to approximately 20–30% increase in the baseline EPSP slope of curve a, upon estradiol perfusion. Red bar above the graph indicates period of time during which estradiol was administered. Acute slices from adult male (3 months) Wistar rats were investigated with a conventional electrophysiological setup. [Modified from Kawato (2004)].

the transient application (3 min) of NMDA. This LTD was induced by the activation of phosphatase due to a moderate Ca^{2+} influx through NMDA receptors (Lee et al., 1998). The plateau EPSP amplitude at 60 min after NMDA application was 80.4% (CA1), 88.8% (CA3) and 95.1% (DG), respectively. A 30 min preperfusion of 10 nM estradiol significantly enhanced LTD resulting in the residual EPSP amplitude at 60 min of 59.7% (CA1), 79.1% (CA3) and 92.2% (DG) (Fig. 2) (Mukai et al., 2007). Investigations using specific estrogen agonists indicated that the contribution of ERα (but not ERβ) was essential to these estradiol effects. Propyl-pyrazole-trinyl-phenol (PPT, ERα agonist) (Harrington et al., 2003) at 100 nM exhibited a significant LTD enhancement in CA1, while diarylpropionitrile (DPN, ERβ agonist) (Harrington et al., 2003) did induce a suppression of LTD in CA1, implying that the contribution of ERβ was opposite to that of ERα in the estradiol effect on LTD. Taken collectively, estradiol-bound ERα may activate phosphatase at moderate Ca^{2+} concentration of around 0.7–1 μM upon 30 μM NMDA application (Yang et al., 1999), and facilitated dephosphorylation of AMPA receptors may induce enhancement of LTD. On the other hand, estradiol-bound ERα is not functional in LTP modulation at high Ca^{2+} concentration of around 5–12 μM under tetanic stimulation (Ishii et al., 2006; Lisman, 1989; Yang et al., 1999), because phosphorylation of AMPA receptors by CaM kinase II is a dominant process at this high Ca^{2+} concentration.

2.2. *Spinogenesis*

Modulation of spinogenesis is another essential action of estrogen in memory processes, involving production of new spines that creates sites for new neuronal contacts. We demonstrated that dendritic spines were rapidly modulated by estradiol application, using single spine analysis of Lucifer-Yellow-injected neurons in adult male hippocampal slices (Komatsuzaki et al., 2005; Tsurugizawa et al., 2005). Following a 2 h treatment with estradiol in the stratum radiatum of CA1 region, the treated dendrites have significantly more spines at 1 nM estradiol (1.31 spines/μm) than dendrites at 0 nM estradiol (0.85 spines/μm) (Fig. 3A) (Mukai et al., 2007). PPT induced a significant enhancement of the spine density to 1.20 spines/μm. However, DPN increased the spine density only slightly (0.95 spines/μm). Blocking of ERα by ICI 182,780 completely suppressed the enhancing effect of estradiol on the spine density. Blocking of phosphorylation of Erk MAP kinase by PD98059 completely prevented the estradiol-induced spinogenesis. Taken together, the enhancement of the spine density is probably induced by activation of Erk MAP kinase by estradiol-bound ERα at the basal low Ca^{2+} concentration of around 0.1–0.2 μM in resting neurons (Ishii et al., 2006). When the Ca^{2+} concentration in spines was further decreased by blocking NMDA receptors with MK-801, the enhancing effect by estradiol was completely suppressed. Function of estradiol-bound ERα therefore needs the basal level of Ca^{2+} concentration of around 0.1–0.2 μM. The morphological changes in CA1 spines occurred by 2 h estradiol treatments. In control slices (0 nM estradiol), the relative population of spines was approximately 24% for mushroom spine, 62% for thin spine, 1% for filopodium and 13% for stubby spine. Upon 1 nM estradiol treatment, the density of thin spine was selectively increased, from 0.57 spines/μm to 0.97 spines/μm, while the density of mushroom and stubby was not significantly altered (Fig. 3A).

The spine density is not always increased but in some cases decreased by the estradiol treatment. The estradiol-induced spinogenesis is highly region specific and heterogeneous. In fact, in CA3 pyramidal neurons, the total density of thorns of thorny excrescencies (spine-like postsynaptic structures in the stratum lucidum of CA3, having contacts with mossy fiber terminals originated from granule cells) decreased dramatically to approximately 70% upon a 2 h treatment of 1 nM estradiol (Fig. 3B) (Tsurugizawa et al., 2005). PPT significantly decreased the density of thorns from 2.19 to 1.66 thorns/μm, but DPN did not significantly change the density of thorns (Fig. 3B). Blocking of Erk MAP kinase by PD98059 completely prevented the estradiol-induced decrease of thorns. Taken together, in the stratum lucidum of CA3, the decrease of the thorn density is probably induced by activation of Erk MAP kinase by estradiol-bound ERα at the basal Ca^{2+} concentration of around 0.1–0.2 μM. When the Ca^{2+} concentration was decreased to below the basal level by blocking AMPA receptors with CNQX, or by changing the outer medium to Ca^{2+}-free ACSF, the suppression effect of estradiol was completely inhibited (Fig. 3B). These results suggest that the decrease of thorns requires the basal Ca^{2+} concentration which is kept by spontaneous postsynaptic Ca^{2+} influx via voltage activated calcium channels depending upon AMPA receptor-mediated spontaneous voltage fluctuations, because the spontaneous Ca^{2+} influx within thorny excrescencies occurs mainly via voltage activated calcium channels (Baude et al., 1995; Fritschy et al., 1998; Monaghan et al., 1983; Reid et al., 2001; Reid, 2002). Note that blocking of NMDA receptors by MK-801 did not prevent the estradiol-induced decrease of thorns. This may be due to much smaller contribution of NMDA receptors to the spontaneous Ca^{2+} influx within thorns than that of voltage activated calcium channels. The function of estradiol-bound ERα therefore needs the basal level of Ca^{2+} concentration around 0.1–0.2 μM.

We always use acute hippocampal slices in order to examine the direct effect of estradiol on glutamatergic neurons within slices. Results from *in vivo* investigations using whole rat may reflect not only direct but also indirect effects of estradiol on glutamatergic neurons via cholinergic or serotonergic neurons, projecting to the hippocampus (MacLusky et al., 2005).

The rapid effect of estrogens has also been observed *in vivo*. Leranth, MacLusky and co-workers have demonstrated that the estradiol (60 μg/kg) increases the spine-synapse density due to synaptic rearrangements in ovariectomized adult rats as rapid as after 30 min of estradiol injection using electron micrographic analysis (MacLusky et al., 2005). On the other hand, over decades, the slow genomic effects (1–4 days) of estradiol on spine plasticity have been extensively investigated *in vivo*. For example, supplement of estrogens in ovariectomized adult female rats (Gould et al., 1990; MacLusky et al., 2005; Woolley et al., 1990; Woolley and McEwen, 1992)

Fig. 2 – Rapid modulation of LTD by 17β-estradiol in hippocampal slices from adult male rats. (Upper CA1, CA3 and DG) Time dependence of maximal EPSP amplitude in CA1 (CA1), CA3 (CA3) and DG (DG). Estradiol concentration was 0 nM (open circle), 1 nM (yellow closed triangle) and 10 nM (red closed diamond), respectively. (Multielectrode) Custom-made 64 multielectrode probe (MED64, Panasonic, Japan) with the hippocampal slice. Stimulation (red circle) and recording (blue circle) electrodes are indicated. Here, 100% EPSP amplitude refers to the EPSP value at $t=-40$ min prior to NMDA stimulation, irrespective of the test condition. LTD was induced by 30 μM NMDA perfusion at time $t=0$ to 3 min (closed bar above the graph). Hatched bar above the graph indicates period of time during which estradiol was administered. The LTD enhancement was reproducibly observed in more than 90 slices out of 100 slices. (Lower CA1, CA3 and DG) Comparison of modulation effect of LTD by 17β-estradiol and agonists in the CA1 (CA1), CA3 (CA3) and DG (DG) of hippocampal slices. Vertical axis is relative EPSP amplitude at $t=60$ min, where EPSP amplitude at $t=60$ min of the control slice without drug application is taken as 100%. From left to right, 17β-estradiol (Estradiol), PPT, DES and DPN at indicated concentrations. Note that coperfusion of 1 μM ICI with 10 nM 17β-estradiol did not suppress the enhancing effect of LTD by estradiol (data not shown). The significance of the estradiol effect was confirmed at 60 min via statistical analysis using ANOVAs ($^*p<0.05$; $^{**}p<0.01$). [Modified from Mukai et al. (2007)].

increases the density of spines in the stratum radiatum of CA1 pyramidal neurons, resulting in recovery of spines to the level of wild rat. These effects of enhancement in spinogenesis have also been observed as rapid as at 4.5 h after s.c. injection of estrogen (MacLusky et al., 2005). *In vitro* investigations have also shown that spine density in CA1 increases following several days' treatment of cultured hippocampal slices with exogenous estradiol (Pozzo-Miller et al., 1999). The contribution of endogenous estradiol has been reported by Rune and co-workers who demonstrated that the suppression of endogenous estradiol synthesis by letrozole treatments for 4 days significantly decreased the spine density in the stratum radiatum of the CA1 region in cultured slices (Kretz et al., 2004).

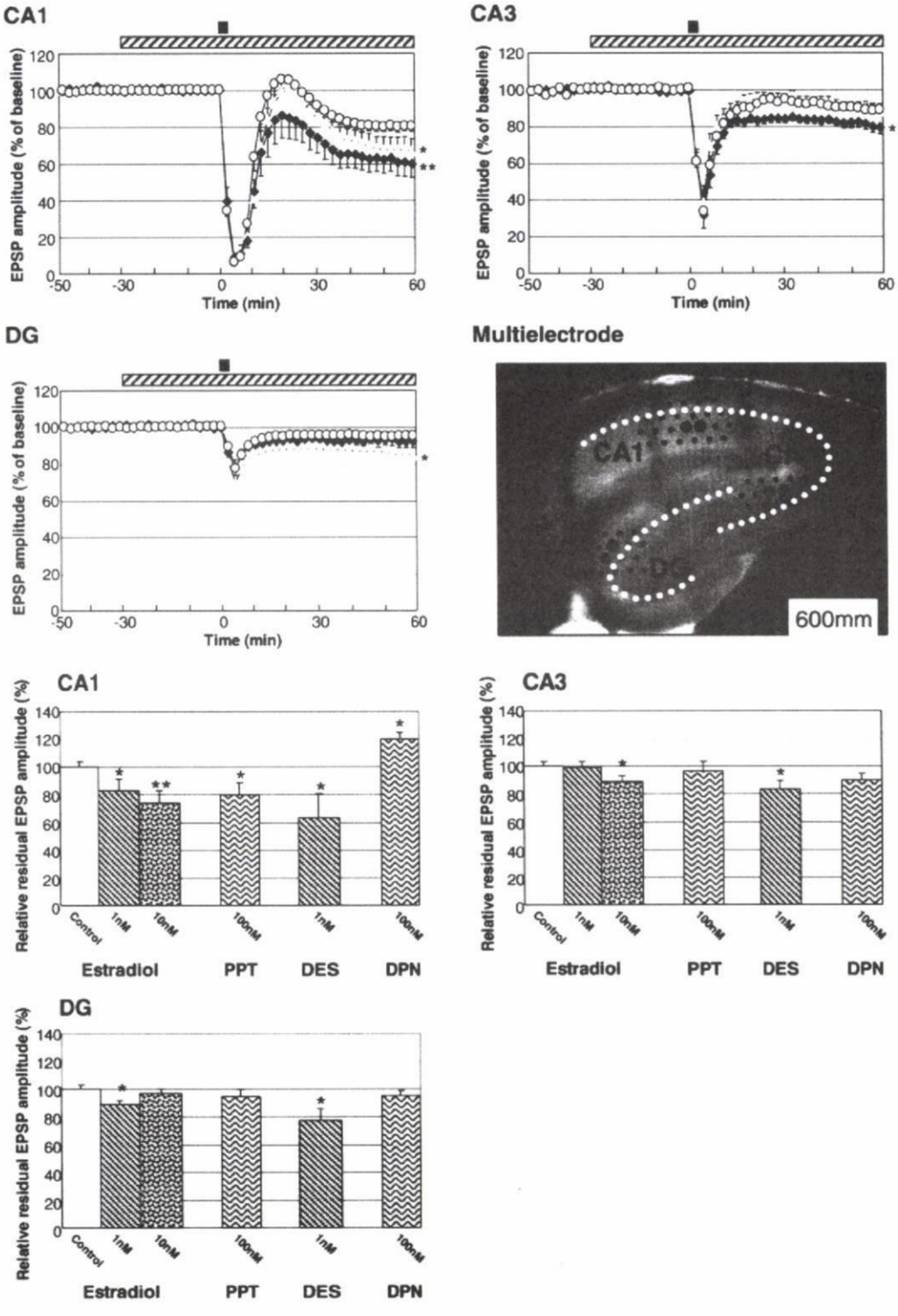

2.3. *Synaptic membrane receptors*

What is the receptor of 17β-estradiol that mediates rapid actions (0.5–2 h) on synaptic plasticity in the hippocampus? Putative synaptic membrane estrogen receptors remain poorly defined. Many attempts have been made to identify membrane estrogen receptors. At the present stage, the most probable candidates for membrane estrogen receptors may be ERα, ERβ and GPR30.

Why are classical nuclear type receptors ERα and ERβ candidates? Because ICI do not suppress estradiol-induced rapid modulation of electrophysiological properties such as LTD, LTP and kinate-induced currents, classical estrogen receptors are suggested to be not involved in these modulations (Gu and Moss, 1996). However, these results do not eliminate the possibility that ERα and ERβ could drive these synaptic transmissions. ICI has been indicated to display its effect by inhibiting dimerization of ERα and ERβ. If dimerization processes are not involved in rapid modulation of electrophysiological phenomena, then ICI cannot block these phenomena. On the other hand, rapid enhancement of spinogenesis via ERα was significantly blocked by ICI (Fig. 3B) (Mukai et al., 2007), therefore dimerization processes occur for synaptic ERα in spinogenesis.

After several years of careful investigations, we successfully identified the membrane estrogen receptor ERα localized in the spines of hippocampal pyramidal and granule neurons by means of immunoelectron microscopic analysis as well as Western blot analysis using affinity-column purified anti-ERα antibody RC-19 (Mukai et al., 2007). A postembedding immunogold electron microscopic analysis demonstrated the synaptic localization of ERα in the glutamatergic neurons in CA1, CA3 and DG (Fig. 4). ERα was also localized in the nuclei. Western blot analysis demonstrated that ERα (67 kDa) and Erk MAP kinase were tightly associated with postsynaptic density fractions (PSD). Because the estradiol-induced modulation of LTD and spine density appeared so rapidly in the time range of 1–2 h, the synaptic ERα observed at PSD and postsynaptic compartments probably plays an essential role in driving rapid processes. It should be noted that specific binding of purified RC-19 antibody to real ERα (67 kDa) in the hippocampus was verified using MALDI-TOF mass-spectrometric analysis of RC-19 reacted proteins as well as the absence of reactivity of RC-19 with ERαKO mice hippocampus (Fig. 5) (Mukai et al., 2007). These analyses are essential in the hippocampus, because we found that non-purified MC-20 antisera, frequently used in previous investigations, often reacted with 62 kDa unknown proteins in the brain and did not significantly react with real ERα (67 kDa) (Mukai et al., 2007). AS409, another frequently used antisera, did mainly react with unknown proteins different from real ERα (Mukai et al., 2007). Non-purified antisera may largely react with proteins having amino acid sequences similar to the real antigen in the hippocampus in which extremely low level of ERα is expressed as compared with that in the ovary (Fig. 6). ERα antisera are normally examined for their reactivity only in endocrine organs such as the ovary in which ERα is highly expressed. Therefore, staining patterns with non-purified antisera probably do not show real ERα distribution in the hippocampus. Antisera should be purified before application to the hippocampus.

ERβ has been reported to associate with membranes in genetically expressed CHO cells and MCF-7 cells (Pedram et al., 2006; Razandi et al., 1999). Several investigations of

Fig. 3 – Changes in the density and morphology of spines in CA1 (A1-A3) or thorns in CA3 (B1-B3) upon treatments of 17β-estradiol (E2) and drugs in hippocampal slices from adult male rats. Spines/thorns were analyzed along the dendrites of pyramidal neurons. (A1) Confocal micrographs showing spines along the secondary dendrites of hippocampal CA1 pyramidal neurons. (Left) A whole image of Lucifer Yellow-injected CA1 neuron. Vertical bar, 100 μm. (Right) Maximal intensity projections onto *XY* plane from *z*-series confocal micrographs, showing spines along the dendrites. From middle to bottom, spines along the apical dendrite in stratum radiatum (Control and E2), and spines along the apical dendrite in stratum lacunosum-moleculare (Control and E2); horizontal bar, 2 μm. Slices were treated in artificial cerebrospinal fluid (ACSF) for 2 h without drugs (Control) or with 1 nM E2 (E2). ACSF contains 2 mM Ca^{2+} and 2 mM Mg^{2+}. (A2) Effect of drug treatments on the total spine density of CA1 neurons in the stratum radiatum (s.r.). Vertical axis is the average number of spines per 1 μm of dendrite. A 2 h treatment in ACSF without drugs (Control), with 1 nM E2 (E2), with 100 nM PPT (PPT), with 100 nM DPN (DPN), with 1 nM E2 and 1 μM ICI 182,780 (ICI+E2), with 1 nM E2 and 20 μM CNQX (CNQX+E2), with 1 nM E2 and 50 μM MK-801 (MK+E2), with 1 nM E2 and 50 μM PD98059 (PD+E2). (A3) Density of 4 subtypes of spines in the CA1 stratum radiatum. A 2 h treatment in ACSF without drugs (Control group), with 1 nM E2 (E2 group), with 100 nM PPT (PPT group), with 1 nM E2 and 1 μM ICI (ICI+E2 group), with 1 nM E2 and 50 μM MK-801 (MK+E2 group), with 1 nM E2 and 50 μM PD98059 (PD+E2 group). In each group, from left to right, mushroom (black column), thin (dotted column), filopodium (hatched column) and stubby (open column). (B1) Maximal intensity projections onto *XY* plane from *z*-series confocal micrographs, showing thorns along the primary/secondary dendrites and spines along the secondary dendrites of hippocampal CA3 pyramidal neurons. (Upper middle) Thorny excrescencies along the primary dendrite in stratum lucidum, scale bar 2 μm. (Upper right) Spines along the apical dendrite in stratum radiatum, scale bar 2 μm. Thorny excrescencies have bulbous-shaped huge heads named thorns (red circles) which are different from spines with separated distribution (yellow circles). (Lower image) A whole image of Lucifer Yellow-injected CA3 neuron. Horizontal bar, 100 μm. (B2) Maximal intensity projections onto *XY* plane from *z*-series confocal micrographs, showing thorns in the CA3 stratum lucidum without drug treatments (control) and thorns after estradiol treatments (E2). Scale bar, 5 μm. (B3) Effect of drug treatments on the average number of thorns per 1 μm dendritic segment in CA3. A 2 h treatment in ACSF without estradiol (control), with 1 nM estradiol (E2), with 100 nM PPT (PPT), with 100 nM DPN (DPN), with 1 nM estradiol and 20 μM CNQX (E2+CNQX), with 1 nM estradiol and 50 μM MK-801 (E2+MK), with 1nM estradiol in ACSF not containing Ca^{2+} (E2 without Ca^{2+}) and with 1 nM estradiol and 20 μM PD98059 (E2+PD). Statistical significance (*$p<0.05$; **$p<0.01$). [Modified from Mukai et al. (2007), Murakami et al. (2006) and Tsurugizawa et al. (2005)].

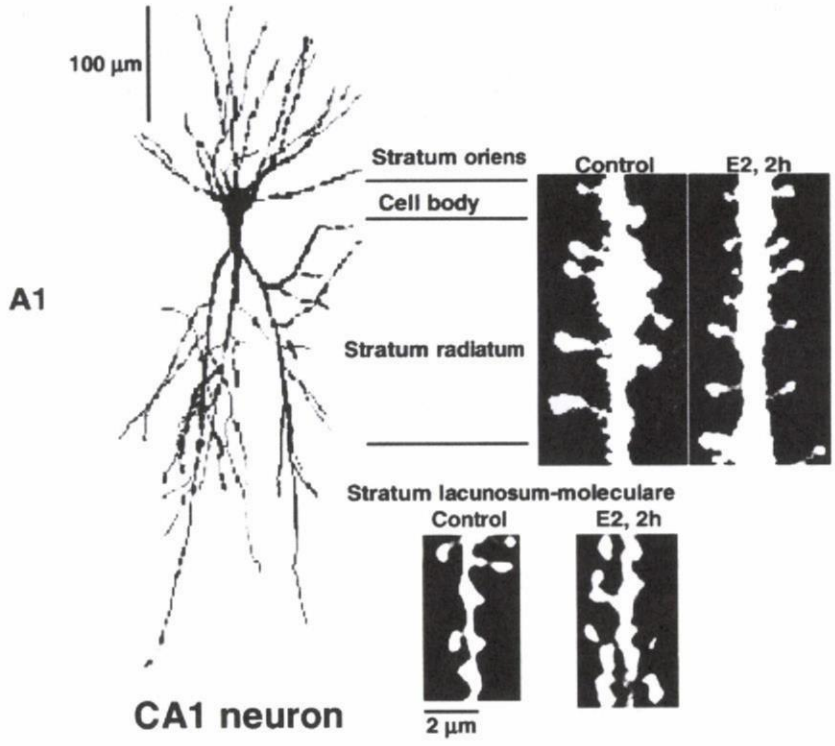

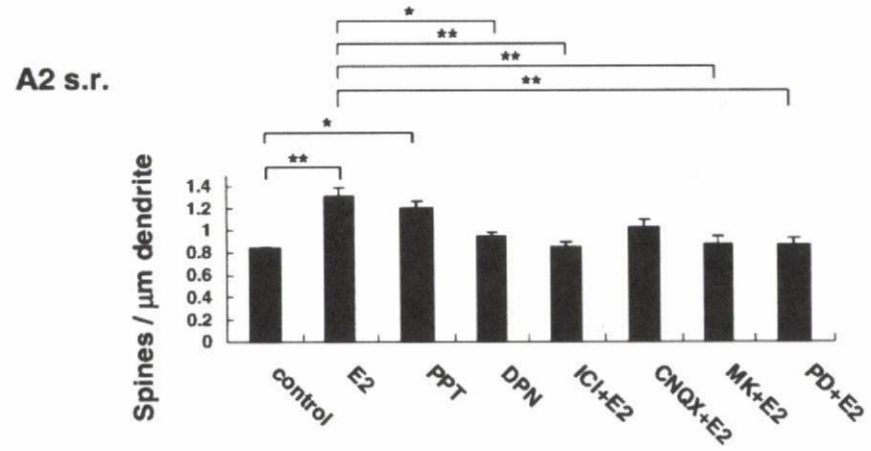

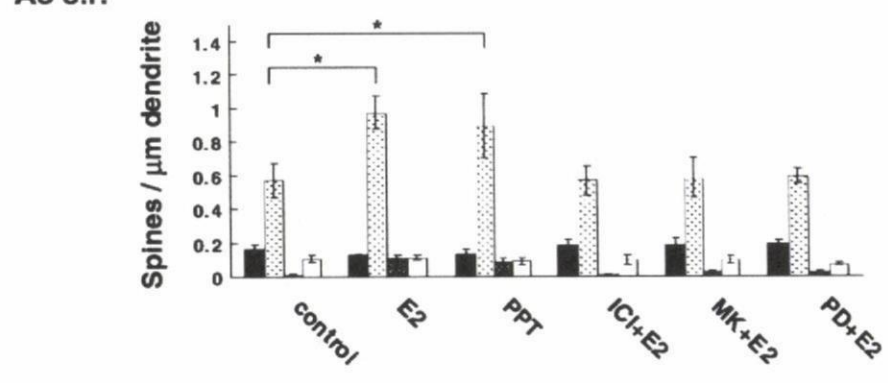

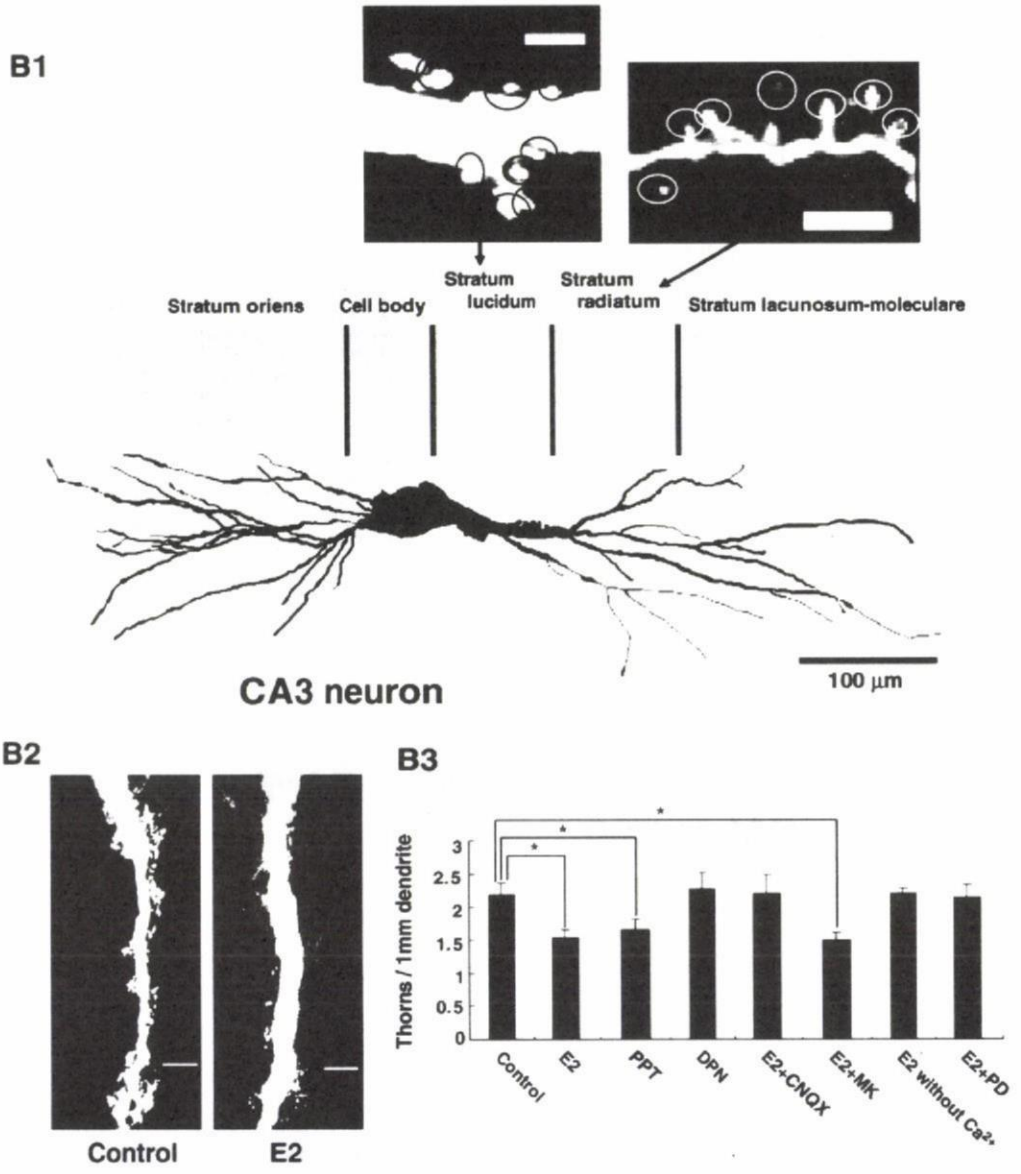

Fig. 3 (*continued*).

immunostaining of ERβ have suggested extranuclear expression of ERβ including dendritic appearance in the hippocampal principal neurons (Milner et al., 2005). ERβ is, however, not yet identified as synaptic membrane receptors. Subcellular immuostaining patterns of these reports might reflect relatively minor expression of ERβ and major expression of unknown proteins, due to multiple reactivity of non-purified ERβ antisera to several unknown proteins in Western blot analysis of hippocampal tissues. The purity of commercially available ERβ antisera may be worse than that of ERα antisera as judged from Western blot analysis.

Recently, transmembrane G-protein coupled estrogen receptor GPR30 has been identified in the plasma membrane of SKBR3 breast cancer cells that lack ERα and ERβ (Thomas et al., 2005) as well as in endoplasmic reticulum membranes of COS7 after genetic expression of GPR30 fused with Green Fluorescent Protein (Revankar et al., 2005). Because expression of GPR30 has also been observed in the hippocampal neurons (Brailoiu et al., 2007), further investigations may reveal its contribution to rapid estradiol modulation of synaptic plasticity.

3. Action of endocrine disrupters on synaptic plasticity

We investigated rapid modulation by endocrine disrupters (low dose of environmental chemicals) of synaptic plasticity in the adult male rat (3 months) hippocampus, by comparison with the estradiol effects (Kawato, 2004). Typical endocrine disrupters were used such as BPA (synthetic material of polycarbonate resin used in dental prostheses, sealants and baby bottles), DES (a synthetic estrogen for preventing miscarriages), nonylphenol and octylphenol (NP and OP, used as surfactants, plasticizers and supplement of resins).

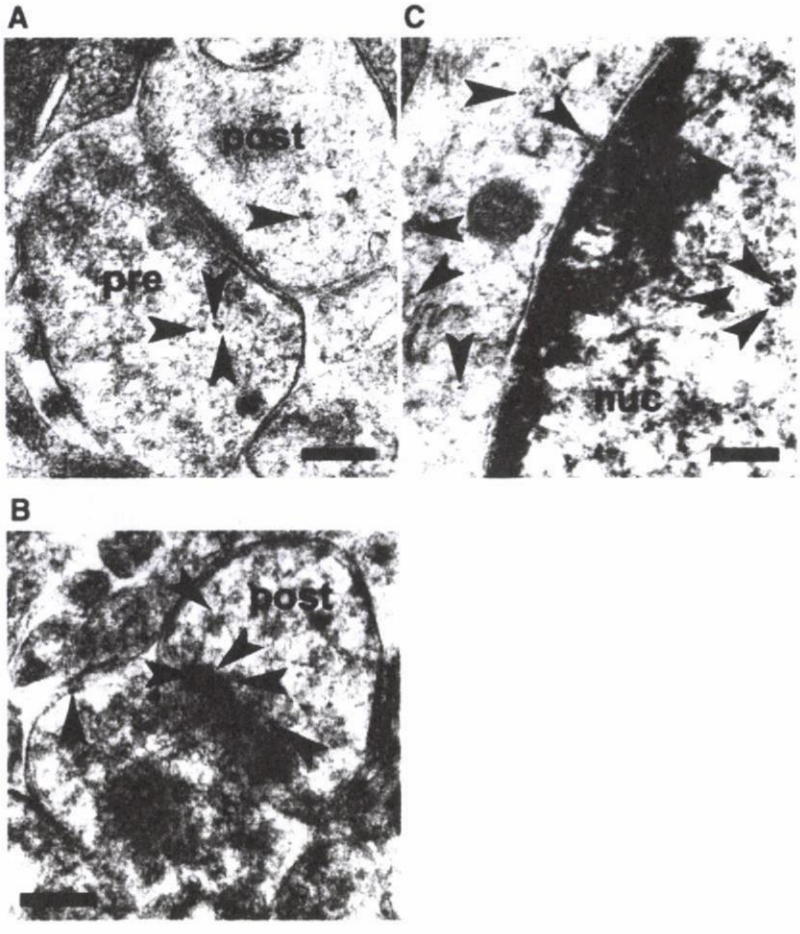

Fig. 4 – Immunoelectron microscopic analysis of the distribution of ERα within axospinous synapses, in the stratum radiatum of the hippocampal slices from adult male rat. (A) Gold particles (arrowheads) were localized in the pre- and postsynaptic regions. (B) In dendritic spines, gold particles were associated with PSD regions. (C) Gold particles were also localized in the nuclei. Pre, presynaptic region; Post, postsynaptic region; Scale bar, 200 nm. [Modified from Mukai et al. (2007)].

The effect of low dose BPA, DES, NP and OP was clearly detectable with the NMDA-induced LTD analysis in CA1, CA3 and DG of the same slices using multielectrode probes (Ogiue-Ikeda et al., 2005; Kawato et al., 2007). A 30 min perfusion of both 10–100 nM BPA and 1 nM DES significantly enhanced LTD in both CA1 and CA3. The percentage of LTD enhancement was 10–20% for BPA and approximately 35% for DES. On the other hand, both 100 nM NP and 100 nM OP suppressed LTD by approximately 10% in CA1 but enhanced by approximately 10% in CA3. In DG, BPA suppressed LTD; however, DES and NP enhanced LTD, while OP did not induce any significant change in LTD. Taken collectively, the effect of endocrine disrupters on LTD was classified into two types, BPA/DES type and NP/OP type. BPA and DES induced the LTD enhancement in CA1 and CA3, which is a similar effect to that of estradiol. NP and OP induced the LTD suppression in CA1 as well as the LTD enhancement in CA3, which is a different effect from that of estradiol.

The effect of endocrine disrupters was also observed on spinogenesis (Tanabe et al., 2005). The density and morphology of dendritic spines were analyzed by imaging Lucifer Yellow-injected CA1 neurons in hippocampal slices. The total spine density was significantly increased by 10 nM BPA and 1 nM DES in the hippocampal CA1. In particular, the thin spine was selectively increased by BPA and DES. These BPA effects are similar to estradiol effects. As additional investigations, a low dose BPA at 10–100 nM transiently increased the intracellular Ca^{2+} level of hippocampal neurons via activation of non-genomic pathway within 20 s (Tanabe et al., 2006).

Is membrane-associated ERα or ERβ a possible receptor for endocrine disrupters? BPA might activate ERα as judged from our results of LTD and spinogenesis. However, the binding affinity of BPA to water soluble ERα has been reported to be much lower (approximately 1/2000) than that of 17β-estradiol (Kuiper et al., 1997). The ligand binding affinity of BPA to ERα has been shown to be 1/100–1/1000 of that of 17β-estradiol (Morohoshi et al., 2005). These reports, however, might not conflict to the reported low dose effect of BPA at nanomolar level, if we take into account the significant concentration processes of BPA in the membrane where membrane bound estrogen receptors exist.

The rapid effect of BPA has also been observed *in vivo*. Leranth, MacLusky and co-workers demonstrated that the estradiol-induced increase in the spine-synapse density was inhibited by the simultaneous application of BPA (40 μg/kg

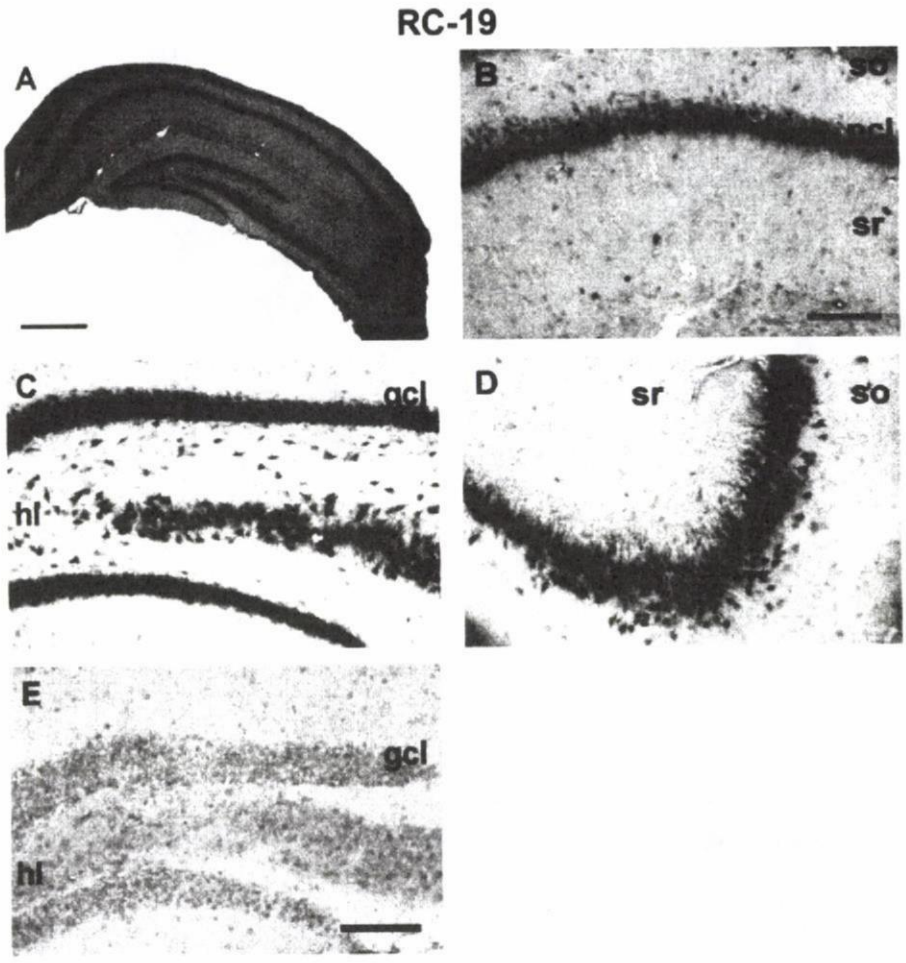

Fig. 5 – Immunohistochemical staining of ERα with RC-19 antibody in the hippocampal slices from adult male rat (A–D) and adult ERαKO mouse (E). (A) Coronal section of the whole hippocampal formation; (B) CA1; (C) DG; (D) CA3; (E) DG of ERαKO mouse. so, stratum oriens; pcl, pyramidal cell layer; sr, stratum radiatum; gcl, granule cell layer; hl, hilus. Scale bar, 500 μm for A, and 200 μm for B–E. [Modified from Mukai et al. (2007)].

body weight) and estradiol (60 μg/kg) in ovariectomized rats for 30 min (MacLusky et al., 2005). It has been also demonstrated that a moderate dosage of 300 μg/kg BPA alone suppressed the spine-synapse density in the CA1 region of the hippocampus in ovariectomized rats (MacLusky et al., 2005). It should be noted that results from *in vivo* investigations may reflect not

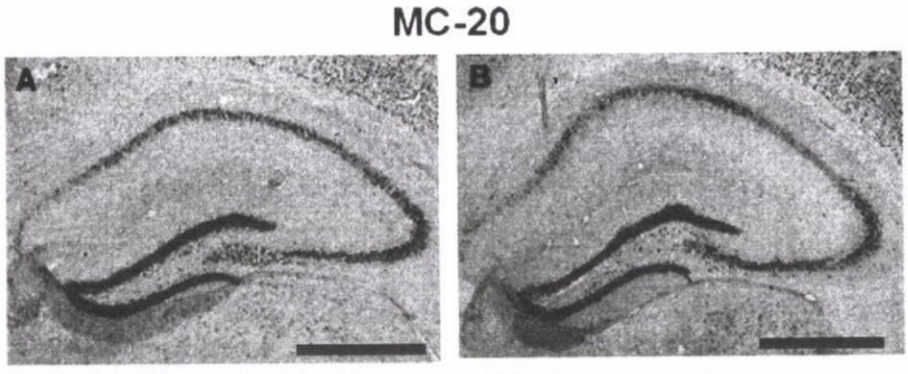

Fig. 6 – Immunohistochemical staining with MC-20 antiserum in the hippocampal slices from adult ERαKO (A) and wild male mice (B). (A and B) The coronal section of the whole hippocampal formation. Scale bar, 50 μm. [Modified from Mukai et al. (2007)].